



Androgen dihydrotestosterone (DHT) promotes the bladder cancer nuclear AR-negative cell invasion via a newly identified membrane androgen receptor (mAR-SLC39A9)-mediated G α i protein/MAPK/MMP9 intracellular signaling

Jinbo Chen^{1,2} · Fujun Chou² · Shuyuan Yeh² · Zhenyu Ou^{1,2} · Chihrong Shyr³ · Chiping Huang³ · Zhendong Xiang² · Yin Sun² · Edward Messing² · Xiongbing Zu¹ · Chawnshang Chang^{2,3}

Received: 22 December 2018 / Revised: 8 May 2019 / Accepted: 15 May 2019 / Published online: 10 September 2019
© The Author(s), under exclusive licence to Springer Nature Limited 2019

Abstract

While androgens may function via nuclear androgen receptor (nAR) to increase bladder cancer (BCa) progression, the impact of androgens on muscle invasive BCa, which contains nearly 80% nAR-negative cells, remains unclear. To dissect the androgens potential impacts on these nAR-negative muscle invasive BCa, we first found that the androgens, dihydrotestosterone (DHT) might function via a novel membrane AR (mAR-SLC39A9) to increase nAR-negative BCa cell migration and invasion. Mechanism dissection revealed that DHT/mAR-SLC39A9 might function by altering G α i protein-mediated MAPK/MMP9 intracellular signaling to increase nAR-negative BCa cell migration and invasion. Preclinical studies using multiple in vitro nAR-negative BCa cell lines and an in vivo mouse model all demonstrated that targeting this newly identified DHT/mAR-SLC39A9/G α i/MAPK/MMP9 signaling with small molecules mAR-SLC39A9-shRNA or G α i-shRNA, and not the classic antiandrogens including enzalutamide, bicalutamide, or hydroxyflutamide, could suppress nAR-negative BCa cell invasion. Results from human clinical samples surveys also indicated the positive correlation of this newly identified DHT/mAR signaling with BCa progression and prognosis. Together, these results suggest that androgens may not only function via the classic nAR to increase the nAR-positive BCa cell invasion, they may also function via this newly identified mAR-SLC39A9 to increase the nAR-negative/mAR-positive BCa cell invasion.

Introduction

Bladder cancer (BCa) is a common urological cancer, which is a major economic burden on health care systems [1]. BCa ranks as the ninth most common malignancy worldwide, and the fifth leading cancer type in the United States [2]. BCa can be divided into two groups: low-grade, papillary and (usually) non-muscle invading (NMI) tumors, which account for the large majority and have a favorable prognosis; and high-grade cancers, over half of which are muscle invading (MI) lesions, and are associated with a poor prognosis [3]. Low-grade NMI BCa can be treated with surgical resection and/or intravesical immunotherapy or chemotherapy, yet 60% of these cancers eventually recur and 10% will eventually progress to MI or metastatic disease [4]. In contrast, about 50% of patients with high-grade MI BCa treated with radical cystectomy and systemic chemotherapy still die from metastases within 2 years of diagnosis [5]. In fact, there has been no major advances in

Supplementary information The online version of this article (<https://doi.org/10.1038/s41388-019-0964-6>) contains supplementary material, which is available to authorized users.

- ✉ Xiongbing Zu
whzuxb@163.com
- ✉ Chawnshang Chang
chang@urmc.rochester.edu

- ¹ Departments of Urology, Xiangya Hospital, Central South University, 410008 Changsha, China
- ² George Whipple Lab for Cancer Research, Departments of Pathology, Urology, Radiation Oncology, and The Wilmot Cancer Center, University of Rochester Medical Institute, Rochester, NY, USA
- ³ Sex Hormone Research Center, Departments of Urology and Medical Technology, China Medical University/Hospital, 404 Taichung, Taiwan

treating MI BCa in the past three decades with no widely recognized second-line therapies [6].

Previous studies have reported that the male to female ratio of BCa incidence is 3 to 1, indicating a greater risk of diagnosing BCa in men than women for both NMI and MI BCa [7]. Accordingly, more men die from BCa than women [8]. One explanation has attributed this gender difference in incidence to sex hormones and their receptors, including the androgen receptor (AR) [9]. The classical nuclear androgen receptor (nAR), which mediates the function of androgens and acts as a transcription factor [10], has been demonstrated to play a key role for the development of BCa in animals [11–13]. However, clinical studies with IHC staining indicate that 30–50% of human BCa specimens failed to express nAR, and nearly 80% of MI BCas were nAR negative [14, 15]. This suggests that loss of nAR expression might be associated with invasive BCa, so that targeting these invasive BCa non-nAR BCa cells with classic antiandrogens like enzalutamide (Enz), bicalutamide (BC), or hydroxyflutamide (HF) may be a questionable strategy.

While most androgens function by binding to the nAR, recent studies indicated that androgens might also be able to function through non-nAR signals, including via intracellular $[Ca^{2+}]$, cAMP, and activation of several downstream genes via G-protein or membrane receptors signals [16–18]. However, very few, if any, studies have linked these non-nAR signals to androgens impact on BCa progression. Here we present the first in vitro and in vivo evidence showing that the androgen, dihydrotestosterone (DHT), can increase migration and invasion of nAR-negative BCa cells via a newly identified membrane AR (mAR-SLC39A9)-mediated intracellular $G_{\alpha i}$ /MAPK/MMP9 signaling.

Results

Testosterone (T) and DHT promote BCa development and progression in a nAR-independent mechanism

Our previous study using BBN-induced BCa development in wild-type (WT) and nAR-knocked-out (nARKO) mice [19] indicated that 92% of the WT male mice developed BCa and none of the nARKO mice developed BCa. However, when nARKO mice were given DHT [19], we found that 25% of the nARKO mice developed BCa [21] (Fig. 1a). Since nARKO mice have little serum androgen and their nAR gene was completely deleted, these in vivo results suggest that the DHT may function through non-nAR signaling to promote BCa development. This is potentially clinically significant since this may represent the first in vivo evidence showing an androgen, in this case DHT,

can also function through non-nAR signaling to promote BCa development and progression.

We then applied multiple approaches to confirm the in vivo discovery in different human nAR-negative BCa cell lines, including J82 and 5637 (Fig. 1b). Results from the “wound-healing” migration assays revealed that androgens, such as DHT and T, substantially increased a migration of these two cell lines into the denuded area (Fig. 1c).

We then used an invasion assay in transwell plates with Matrigel-coated filters and the results confirmed that 10 nM T or DHT significantly increased invasion by the nAR-negative J82 and 5637 BCa cells (Fig. 1d). Furthermore, adding nAR-shRNA to these nAR-negative J82 and 5637 cells also showed little impact on DHT-increased cell migration and invasion (Supplementary Fig. 1A, B). In contrast, in the nAR-positive UMUC3 cells, nAR-shRNA suppressed DHT-induced cell migration and invasion (Supplementary Fig. 1C–E).

Importantly, we found that treating with various antiandrogens, including Enz, BC, and HF, all failed to suppress the DHT-increased cell migration and invasion in J82 and 5637 cells that express little nAR (Fig. 1e, f). In contrast, we found these antiandrogens could significantly suppress DHT-increased cell migration and invasion in the UMUC3 BCa cells that express the nAR (Supplementary Fig. 2A, B).

Together, results from Fig. 1a–f and Supplementary Fig. 1 and 2 are in agreement with our initial in vivo data in the nARKO mice showing androgens, including T and DHT, can increase BCa nAR-negative cell migration and invasion, and the current antiandrogens failed to suppress these androgenic effects.

DHT increases the BCa nAR-negative cell invasion: via mAR-SLC39A9

The above in vivo mouse and in vitro human cell line results indicated that androgens might function through some unidentified receptor(s) to increase the BCa nAR-negative cell invasion. We then focused on screening some G-protein-coupled receptors (GPCRs) and membrane receptors that were potentially able to mediate steroid hormone function [18, 20–24]. We found that expression of two GPCRs, SLC39A9 and GPRC6A, could be detected (with much lower expression of GPRC6A) in both nAR-negative J82 and 5637 BCa cells (Fig. 2a). A survey of BCa patients from the TCGA database also found that SLC39A9 expression is abundant. In contrast, expression of GPRC6A is relatively low in TCGA BCa patient samples (Fig. 2b). We therefore focused on this membrane AR, GPCR-SLC39A9 (named as mAR-SLC39A9) for further analyses.

We first tested mAR-SLC39A9 protein expression in multiple human BCa cell lines (T24, J82, 5637, and

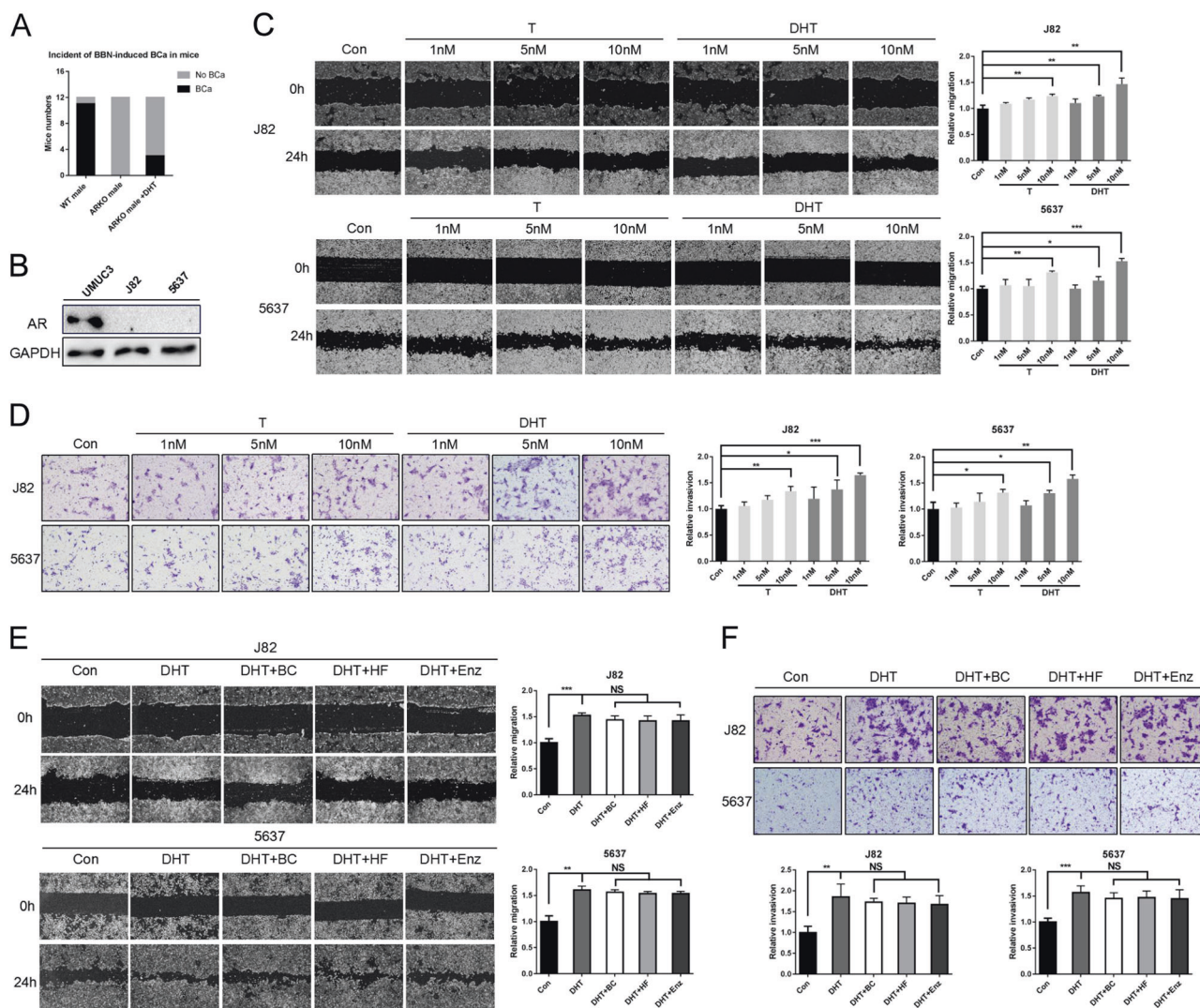


Fig. 1 DHT effects on migration and invasion of BCa nAR-negative J82 and 5637 cells. **a** Incidence of BBN-induced BCa in WT and nARKO mice treated with or without DHT, showing 25% of nARKO mice developed BCa after DHT supplementation (these data were rearranged from Table 1 of our previous paper [19]). **b** Western blot verification of AR protein expression in J82 and 5637 cells, compared with UMUC3 cells. **c** Cell migration of urothelial cancer cells was evaluated by wound-healing assay for in vitro closure of a wound. The BCa cells were plated at high density to grow into confluency, confluent cells were then wounded, and incubated for migration for additional 24 h in the absence or presence of DHT. In vitro wound-healing motility assay for testosterone (T) at 1, 5, or 10 nM and DHT

at 1, 5, or 10 nM in J82 and 5637 cells. **d** Transwell invasion assays (diagram) were performed. Cells that had invaded to the lower surface of the filter were counted and averaged from ten randomly chosen microscopic fields (100 ×). Transwell assay for T at 1, 5, or 10 nM and DHT at 1, 5, or 10 nM in J82 and 5637 cells. **e** Wound-healing assay for DHT plus antiandrogens bicalutamide (BC) at 10 μM, hydroxyflutamide (HF) at 5 μM and enzalutamide (Enz) at 10 μM in J82 and 5637 cells. **f** Transwell assay for DHT plus antiandrogens in J82 and 5637 cells. For **c**, **d** and **e** quantitations are on the right. The values are the means ± SD from at least three independent experiments. **P* < 0.05 compared with corresponding vehicle control, ***P* < 0.01, ****P* < 0.001, NS = not significant

UMUC3) vs. the normal human bladder epithelial cell line SVHUC, and found its expression was elevated in BCa cell lines (Fig. 2c). Then, we applied interruption approaches using two specific shRNAs to block mAR-SLC39A9 expression (see their suppressing effects on the protein level in Fig. 2d), and results revealed that suppressed mAR-SLC39A9 expression blocked DHT-increased cell migration (Fig. 2e) and invasion (Fig. 2f) in nAR-negative J82

and 5637 BCa cells. We then applied the opposite approach by adding mAR-SLC39A9-cDNA (Fig. 2g), and results revealed that increased mAR-SLC39A9 expression also increased DHT stimulation of cell migration (Fig. 2h) and invasion (Fig. 2i) in J82 and 5637 cells.

Together, results from Fig. 2a–i suggest that DHT may function through mAR-SLC39A9 to increase cell migration and invasion in nAR-negative J82 and 5637 BCa cells.

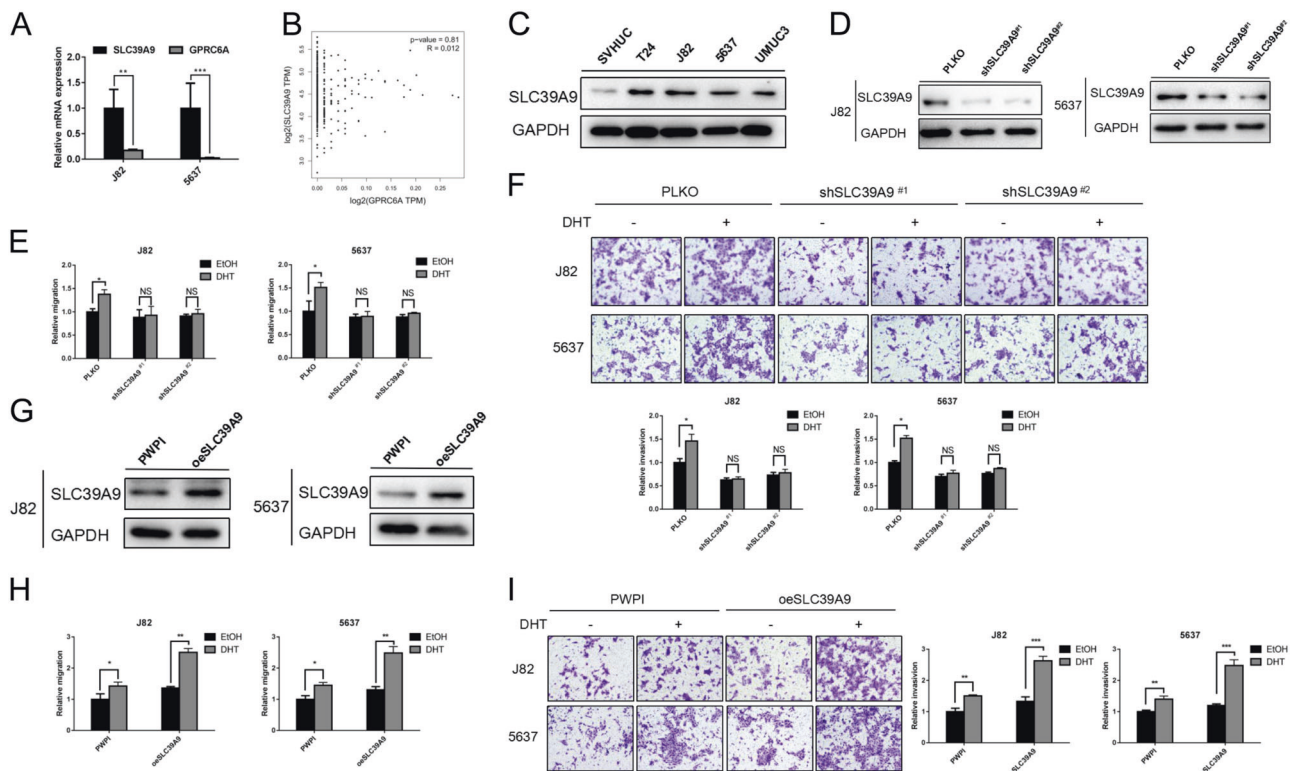


Fig. 2 The membrane G-protein-coupled receptor, SLC39A9, mediated the DHT-enhanced cell migration/invasion in nAR-negative BCa cells. **a** Real-time PCR assay validation of SLC39A9 and GPRC6A mRNA expression in BCa J82 and 5637 cell lines. **b** Relative mRNA expression of SLC39A9 and GPRC6A in BCa samples from the TCGA database. **c** Western blot validation of mAR-SLC39A9 protein expression elevation in multiple BCa cell lines (T24, J82, 5637, and UMUC3) vs. normal bladder epithelial cell line, SVHUC. **d** The protein level of SLC39A9 was decreased when knocked down using shSLC39A9^{#1} and shSLC39A9^{#2} in J82 and 5637 cells. **e** Migration assay after using two specific shRNAs for SLC39A9 in J82 and 5637

cells treated with/without DHT or PLKO.1-vector (PLKO) as control. **f** Transwell assays were performed after using shSLC39A9 in J82 and 5637 cells treated with/without DHT or PLKO as control. **g** Western blot validated SLC39A9 was overexpressed when using SLC39A9-cDNA in J82 and 5637 cells. **h** Migration assays after SLC39A9 overexpression in J82 and 5637 cells treated with/without DHT or PWPI as control. **i** Transwell assays after SLC39A9 overexpression in J82 and 5637 cells treated with/without DHT or PWPI. For **f** and **i** quantifications are below or to the right, respectively, of the images. The values are the means \pm SD from at least three independent experiments. * $P < 0.05$, ** $P < 0.01$, *** $P < 0.001$, NS = not significant

DHT/mAR-SLC39A9 signaling increases the nAR-negative BCa cell invasion via altering G α i protein signaling

Most GPCRs function through one G protein (small G proteins or larger G proteins that are made up of α , β , and γ subunits) to link extra-cellular stimulation to intracellular signals [25, 26]. Previous studies indicated SLC39A9 might function via a coupled G α i protein to mediate MAP kinase signaling to stimulate prostate cancer progression [23]. To identify which G protein can mediate the DHT/mAR-SLC39A9 signaling to increase nAR-negative BCa cell invasion, we utilized immunoprecipitation of membrane-bound [³⁵S]-GTP γ S with specific G α antibodies to demonstrate that [³⁵S]-GTP γ S level was increased after 10 nM DHT treatment only in the G α i group and not in the G α s group in J82 and 5637 cells (Fig. 3a).

In addition, results from multiple interruption approaches with different shRNAs, or treated with specific inhibitors of

those individual G proteins to examine whether any interruption of DHT/mAR-SLC39A9 could alter cell invasion. And these data revealed that treating with 100 ng/ml pertussis toxin (PTX), a specific inhibitor that can selectively block G α i protein (via ADP ribosylation on the α subunit of the G protein to interrupt the formation of the G protein heterotrimer with GPCRs [27]), blocked DHT-increased cell migration and invasion (Fig. 3b, c) in J82 and 5637 cells.

We further used a second interruption approach to confirm the first interruption result using shRNA with three subunits of G α i (shG α i1, shG α i2, and shG α i3, see reduced G α i mRNA expression in Fig. 3d), and found that blocking G α i with multiple G α i-shRNAs all or partly blocked/interrupted the DHT-increased J82 and 5637 cell migration and invasion (Fig. 3e, f). Importantly, the co-immunoprecipitation (CO-IP) assay revealed SLC39A9 protein could directly bind with G α i (Fig. 3g).

Together, results from Fig. 3a–g using different approaches with different inhibitors all demonstrated that DHT/

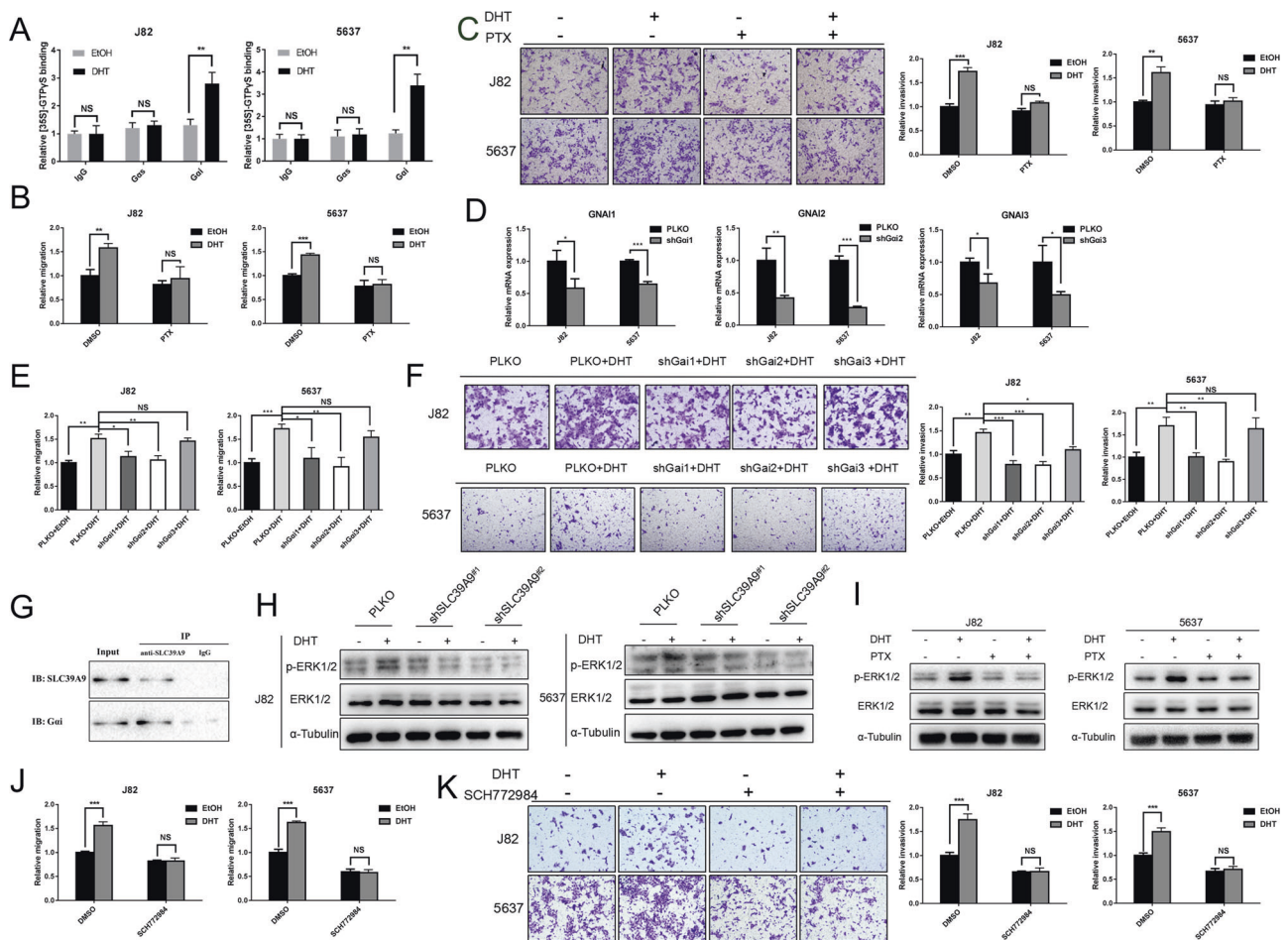


Fig. 3 The DHT/mAR-SLC39A9/ $G_{\alpha i}$ signaling mediated the MAPK family ERK1/2 activation to promote BCa cell migration/invasion in nAR-negative BCa cells. **a** Immunoprecipitation of membrane-bound [35S]-GTP γ S bound to G protein α subunits on plasma membranes activated by 10 nM DHT treatment with specific G protein α subunit antibodies or control IgG. **b–c** DHT-increased migration (**b**) and cell invasion (**c**) effects in J82 and 5637 cells were blocked by 100 ng/ml pertussis toxin (PTX) treatment. **d** The qPCR result for $G_{\alpha i}$ after using specific three subunits of $G_{\alpha i}$ -shRNA (shG αi 1, shG αi 2, and shG αi 3) in J82 and 5637 cells. **e–f** DHT-increased migration (**e**) and effect on the cell invasion (**f**) in J82 and 5637 cells was partly blocked after

knocking down $G_{\alpha i}$. **g** Co-precipitation of SLC39A9 and $G_{\alpha i}$ protein. Western Blot for MAPK family ERK1/2 and p-ERK1/2 expression using sh-SLC39A9 (**h**) with/without DHT, α -tubulin as an internal control. **j** Migration assays showed 0.1 μ M ERK1/2 inhibitor SCH772984 could block DHT-induced cell migration in J82 and 5637 cells. **k** Transwell assays showed 0.1 μ M ERK1/2 inhibitor SCH772984 could block DHT-induced cell invasion in J82 and 5637 cells. For **c**, **f**, and **k**, quantitations are on the right, respectively of the images. The values are the means \pm SD from at least three independent experiments. * P < 0.05, ** P < 0.01, *** P < 0.001, NS = not significant

mAR-SLC39A9 signaling may function by altering $G_{\alpha i}$ protein to increase nAR-negative BCa cell invasion.

The DHT/mAR-SLC39A9/ $G_{\alpha i}$ signaling can increase the nAR-negative BCa cell invasion via increasing MAPK family ERK1/2 phosphorylation signaling

Next, to search for the intracellular downstream signals that mediate DHT/mAR-SLC39A9/ $G_{\alpha i}$ -increased nAR-negative BCa cell invasion, we focused on the MAPK family ERK1/2 signals since early studies indicated the SLC39A9 could modulate MAPK signaling to influence the behavior of prostate and breast cancer cells [22, 28].

We first demonstrated that treatment with 10 nM DHT activated MAPK family ERK1/2 phosphorylation in BCa cell lines. We then added mAR-SLC39A9-shRNA or treated with the $G_{\alpha i}$ inhibitor PTX, and demonstrated that both resulted in decreased phosphorylation of MAPK family ERK1/2 (Fig. 3h, i). Importantly, treating with 0.1 μ M SCH772984, an inhibitor specific for ERK1/2, could then block/interrupt DHT-enhanced BCa cell migration (Fig. 3j) and invasion (Fig. 3k) in both nAR-negative J82 and 5637 cells.

Together, results from Fig. 3h to k suggest that the DHT/mAR-SLC39A9/ $G_{\alpha i}$ signaling may function via increasing the MAPK family ERK1/2 phosphorylation, which can then increase the nAR-negative BCa cell invasion.

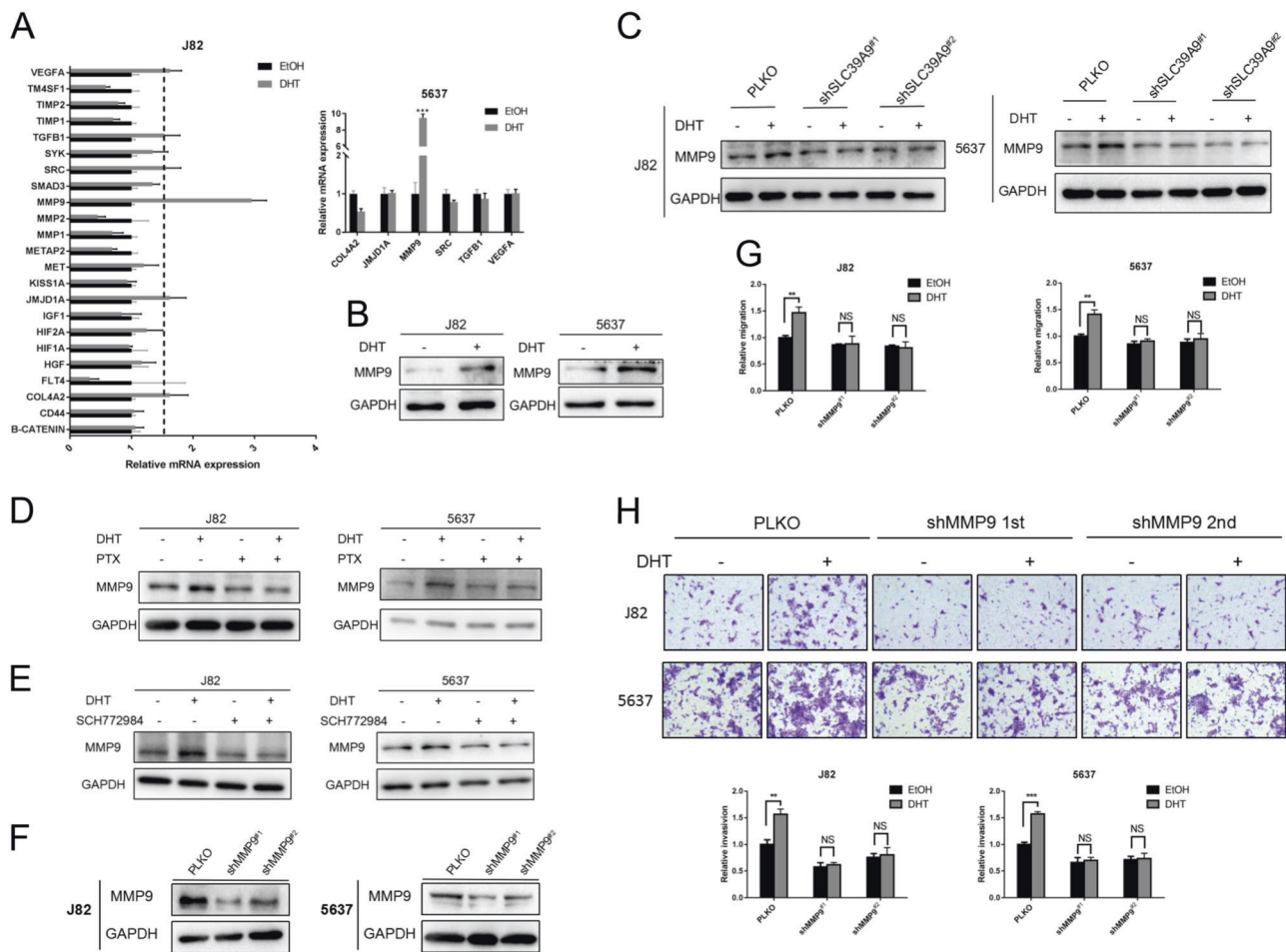


Fig. 4 a The qRT-PCR assay for screening some metastasis genes after treating J82 cells with 10 nM DHT. Candidate genes with a fold change of ≥ 1.5 were then analyzed in 5637 cells. **b** Representative western blot analysis of MMP9 levels in J82 and 5637 cells treated with/without 10 nM DHT/ETOH. **c** Western blot of MMP9 via adding SLC39A9-shRNA treated with/without 10 nM DHT/ETOH. **d-e** Western blot of MMP9 treated with G_{αi} inhibitor (**d**) 100 ng/ml Pertussis toxin (PTX) or ERK1/2 inhibitor (**e**) 0.1 μ M SCH772984.

f Western blot to show MMP9 knockdown efficiency in J82 and 5637 cells. **g** Migration assay using shMMP9^{#1} and shMMP9^{#2} in J82 and 5637 cells treated with/without 10 nM DHT. **h** Transwell assay after sh-MMP9 in J82 and 5637 cells treated with/without 10 nM DHT. For **h**, quantitations are below the images. The values are the means \pm SD from at least three independent experiments. ** $P < 0.01$, *** $P < 0.001$, NS = not significant

The DHT/mAR-SLC39A9-Gai/MAPK signaling increases the nAR-negative BCa cell invasion via increasing MMP9 expression

To search for the potential downstream genes that can mediate DHT/mAR-SLC39A9/G_{αi}/MAPK-increased nAR-negative BCa cell invasion, we then screened several metastases related genes expressed in both J82 and 5637 cells. We found that 10 nM DHT increased the mRNA expression of the pro-metastasis gene, MMP9, in nAR-negative J82 and 5637 BCa cells (Fig. 4a). Western blot analyses further confirmed MMP9 protein expression was increased after treating with 10 nM DHT in these cells (Fig. 4b).

We therefore focused on MMP9 since both its mRNA and protein expressions were increased after treating cells with 10 nM DHT. The interruption approaches via adding mAR-SLC39A9-shRNA, or treating with G_{αi} inhibitor PTX or ERK1/2 inhibitor SCH772984, all resulted in reduced MMP9 expression at the protein level (Fig. 4c-e). Importantly, adding MMP9-shRNAs, which significantly suppressed MMP9 expression (Fig. 4f), blocked DHT-induced cell migration and invasion in J82 and 5637 BCa cells (Fig. 4g, h).

Together, results from Fig. 4a-h suggest that the DHT/mAR-SLC39A9/G_{αi}/MAPK signaling may function by increasing the expression of the metastasis-related gene, MMP9, which may then increase nAR-negative BCa cell invasion.

Preclinical study using an in vivo mouse model to confirm that DHT functions via altering the mAR-SLC39A9/G_{αi}/MAPK/MMP9 signaling to increase BCa metastasis

To confirm the in vitro cell line data in the in vivo mouse model, we first castrated BALB/c nude mice to remove androgens and then orthotopically xenografted AR-negative BCa J82 cells expressing firefly luciferase into mouse bladder walls and treated mice with DHT or ETOH (see outline in Fig. 5a). After 6 weeks of implantation, the mice were killed, and the primary tumors and metastatic sites were examined. The results indicated that mice receiving DHT injections developed significantly more metastatic tumors than the ETOH control group (Fig. 5b, c). Importantly, in two mouse groups, using the small molecules, mAR-SLC39A9-shRNA or G_{αi}-shRNA to suppress DHT/mAR-SLC39A9/G_{αi} signaling in the injected cells, both BCa progression and metastasis are suppressed (Fig. 5d, e). The quantitative real-time PCR (qRT-PCR) results confirmed knock down of SLC39A9 and G_{αi} in mice tumor tissues were successfully established (Fig. 5f, g).

Immunohistochemical (IHC) staining also found that the expressions of p-ERK1/2, MMP9, were higher in tumors of DHT-treated mice compared with the ETOH controls. Using the small molecules, mAR-SLC39A9-shRNA or G_{αi}-shRNA to suppress mAR-SLC39A9/G_{αi} signaling, suppressed DHT-increased p-ERK1/2/MMP9 signaling (Fig. 5h).

Together, preclinical studies from the in vivo BCa mouse model in Fig. 5a–f are in agreement with in vitro cell line data showing DHT can increase BCa metastasis via altering DHT/mAR-SLC39A9/G_{αi}/ERK1/2/MMP9 signaling in the nAR-negative BCa cells.

Human clinical studies for mAR-SLC39A9 expression in BCa patients

Finally, to link all of the in vitro and in vivo results presented above to human clinical samples, we analyzed human clinical data from the TCGA database. Results showed that mAR-SLC39A9 mRNA expression is higher in BCa tissue samples compared with para-tumor tissues ($P = 0.001$) (Fig. 6a). In addition, mAR-SLC39A9 mRNA expression correlated inversely with overall survival (OS) and disease-free survival (DFS) in BCa patients; higher expression of mAR-SLC39A9 is associated with a poorer prognosis from BCa ($P = 0.008$ and 0.003 , respectively) (Fig. 6b).

Importantly, in 63 human BCa samples IHC staining revealed that moderate to strongly positive (++, +++) mAR-SLC39A9 expression was seen in 57.14% (36/63) of cases, while the positive nAR expression (+, ++, +++) was

present in 20.63% (13/63) of cases. Furthermore, we found 62.00% (31/50) of nAR-negative BCa tissues had moderately to strongly positive expression (++, +++) of mAR-SLC39A9 (Fig. 6c–e). Clinicopathologic correlation also showed that mAR-SLC39A9 expression was directly associated with BCa pathological stage, pathological grade, and presence of lymph node metastasis ($P = 0.043$, 0.012 , 0.021 , respectively) (Supplementary Table 1). These results indicate that more than half of nAR-negative BCa tumors in patients may have moderately to strongly positive mAR-SLC39A9 expression that can mediate androgen induced tumor invasion and progression. Unfortunately, all antiandrogens tested have little ability to suppress this newly identified DHT/mAR-SLC39A9/G_{αi}/ERK1/2/MMP9 signaling.

Discussion

Androgens function mainly through binding to the classical nAR, a transcription factor that functions via transactivating various downstream genes [10, 29, 30]. Indeed, in addition to the classical nAR, earlier studies revealed androgens could also stimulate second messenger cascades increasing intracellular [Ca²⁺], cAMP, through a GPCR, or be functionally linked to a membrane receptor [16, 31, 32]. Recently, two mARs were identified in multiple cell lines. GPRC6A is a PTX-sensitive member of the C family of GPCRs [21] and Pi et al. found it was a novel molecular target for regulating prostate cancer growth and progression [33]. Another mAR is SLC39A9 (also named ZIP9), which is coupled to G proteins [34] and Thomas et al. found it is upregulated in malignant breast and prostate tissues and mediates apoptotic actions of androgens [22]. They also demonstrated SLC39A9 is a specific G_i coupled-GPCR that mediates T-induced MAPK and zinc signaling in prostate cancer cells [23]. However, very few, if any, in vivo studies documented a link between androgens and mAR-SLC39A9 signals in animal studies.

Here we found two potential mARs, GPRC6A and SLC39A9, whose expression could be detected (with much lower expression for the GPRC6A) in both J82 and 5637 cells. The clinical survey from the TCGA database also found that SLC39A9 expression is more abundant than GPRC6A in human BCa tissue samples. We therefore focused on mAR-SLC39A9 for further analysis. Preclinical studies using multiple nAR-negative BCa cells in vitro and in an in vivo mouse model demonstrated androgens might function via mAR-SLC39A9 to increase nAR-negative BCa cell migration and invasion. Furthermore, in addition to the TCGA database, the Oncomine database also indicated that mAR-SLC39A9 expression was elevated in NMI BCa vs. normal bladder tissues (Dyrskjot Bladder 3 dataset), and increased in MI vs. NMI

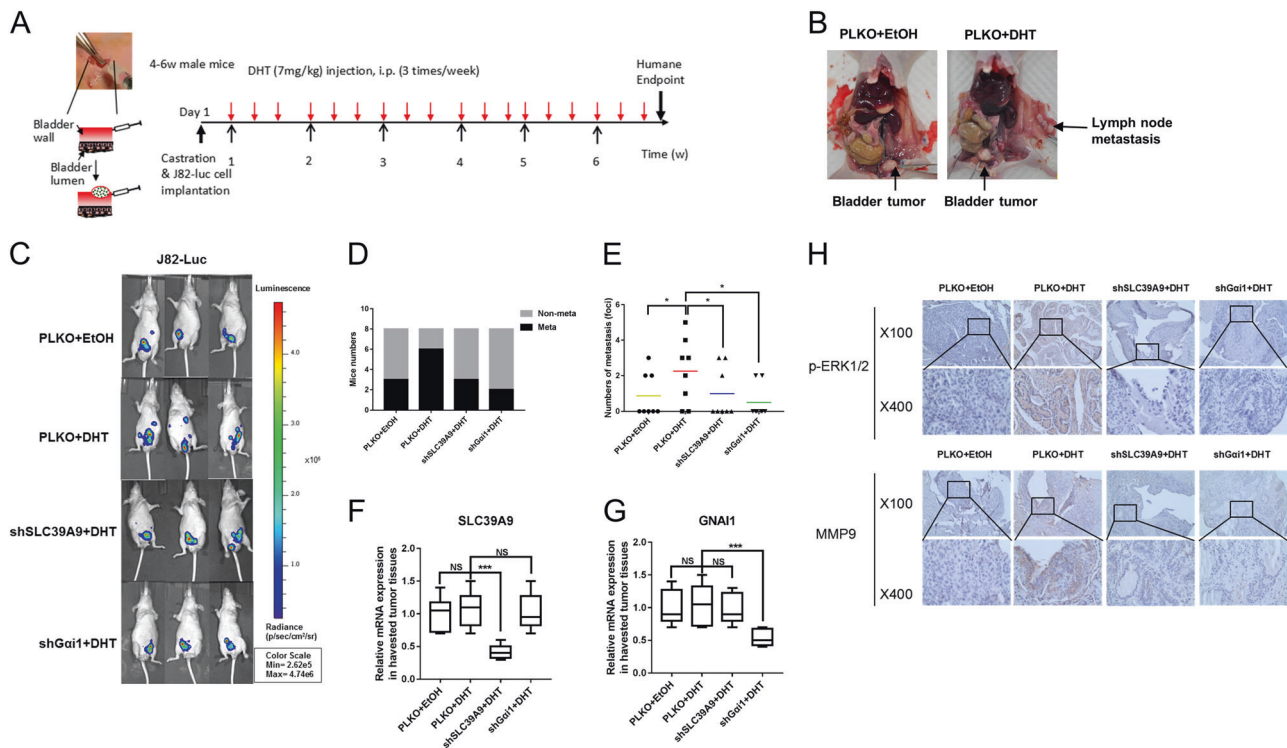


Fig. 5 Preclinical study using the mouse model to confirm DHT-increased BCa metastasis via mAR-SLC39A9/G α _i/ERK/MMP9 axis in nAR-negative BCa cells. **a** The experimental scheme. The tumor metastases in castrated nude mice implanted with J82-Luc cells transplanted with PLKO-vector, PLKO-SLC39A9-shRNA, or PLKO-G α _i1-shRNA. The nude mice were divided into four groups for cell line injections and treated with/without DHT/EtOH: PLKO-vector+EtOH (Mock), PLKO-vector + DHT, PLKO-SCL39A9-shRNA + DHT, PLKO-G α _i1-shRNA+DHT, and IVIS performed weekly for 6 weeks.

Mice were killed after 6 weeks and assessed for bladder tumors and metastases. **b** The representative pictures of lymph node metastases. **c** Representative IVIS images of tumors and metastases. **d** Numbers of mice with/without Metastasis in the four groups. **e** Number of metastasis foci in each group. **f–g** The expression of knocking down of SLC39A9 (**f**) and G α _i1 (**g**) in mice tumor tissues. **h** Representative IHC images and quantification of p-ERK1/2 and MMP9 expression in mice primary bladder tumors of the four groups. The values in **e**, **f**, and **g** are the means \pm SD. * $P < 0.05$, *** $P < 0.001$, NS = not significant

BCa samples (Sanchez-Carbayo Bladder 2 dataset) (Supplementary Fig. 3).

Interestingly, results from recent clinical studies also supported our findings showing that androgen-deprivation-therapy via reducing androgens using an LHRH analog could reduce BCa incidence and recurrence [35]. A separate study also indicated that ADT with an LHRH analog reduces BCa morbidity in patients with prostate cancer while both surgery and radiation therapy failed to do so [36]. Importantly, there are also ongoing clinical trials studying the antiandrogen Enz in combination with gemcitabine and cisplatin in advanced urothelial cancer (NCT02300610) [11].

Our current findings may have significant clinical implications on those human clinical trials. It is likely that antiandrogens, including Enz, may only have beneficial results for those BCa patients whose BCa expresses the nAR. However, since nearly 80% of invasive BCAs are nAR negative [14, 15], our results would predict little benefit of Enz in these patients. In contrast, if ADT with Enz therapy

was replaced with a combination of anti-nAR plus anti-mAR-SLC39A9 treatment or one that directly reduces androgen biosynthesis from the testis (e.g., using a LHRH analog) or from adrenal glands (e.g., using Abiraterone), may have better therapeutic effects to suppress BCa progression. Our studies revealed that DHT-mAR-SLC39A9 might function via altering G α _i protein-mediated ERK1/2-MAPK/MMP9 signaling to increase migration and invasion of the nAR-negative BCa cells. This is in agreement with previous work showing that G protein activation could alter intracellular MAPK signaling [37], and MAPK activation by phosphorylation could also increase the expression of the pre-metastatic gene MMP9, which may play vital roles in progression of multiple cancers [38–40].

In conclusion, our preclinical studies using multiple in vitro cell lines and an in vivo mouse model, as well as human clinical specimens, all suggest that androgens may function via mAR-SLC39A9/G α _i signaling to increase the nAR-negative BCa cell invasion (Fig. 7). Targeting the newly identified DHT/mAR-SLC39A9/G α _i/MAPK/MMP9 signaling

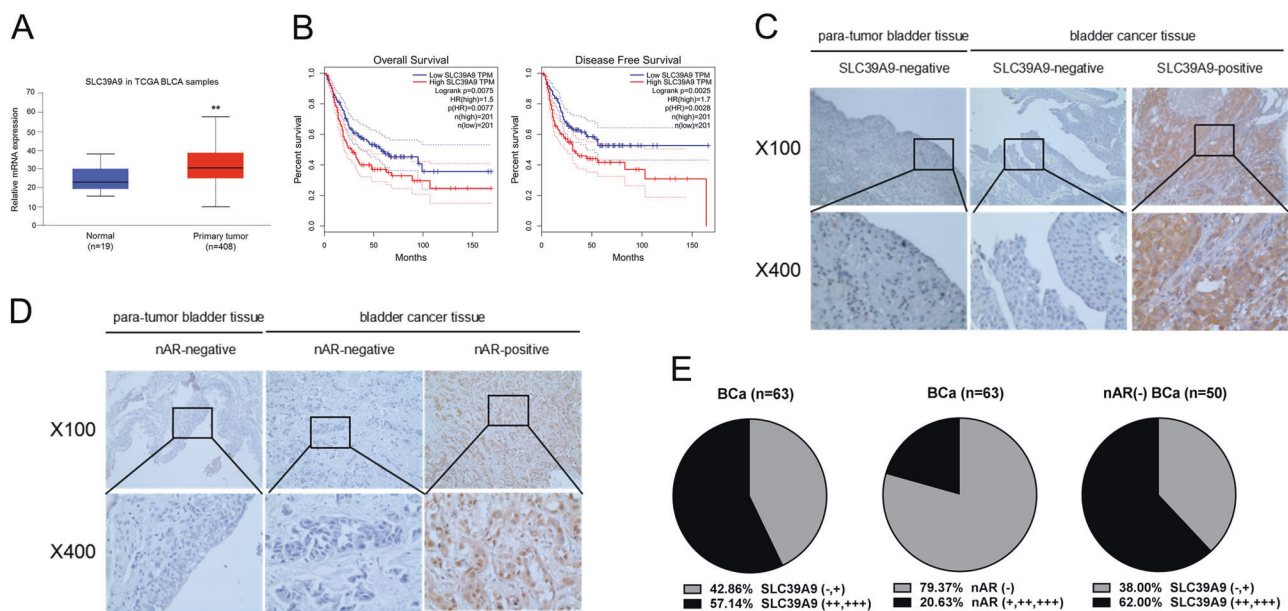


Fig. 6 Human clinical studies for mAR-SLC39A9 expression in BCa patients. **a** TCGA database analysis revealed SLC39A9 expression is higher in BCa tissue samples ($n = 408$) compared with para-tumor tissues ($n = 19$) ($P = 0.001$). **b** Overall survival (OS) and disease free survival (DFS) analysis for SLC39A9 mRNA expression in BCa patients ($P = 0.008$ and 0.003 , respectively). SLC39A9 mRNA levels

were separated to lower than 50% ($n = 201$) vs. higher than 50% ($n = 201$). Representative IHC image of mAR-SLC39A9 **c** and AR **d** expression in BCa and para-tumor tissue samples. **e** Positive rates of mAR-SLC39A9 ($n = 63$) (left) and AR expression in BCa samples ($n = 63$) (middle), as well as mAR-SLC39A9 expression in AR-negative BCa samples ($n = 50$)

with small molecules may provide new therapies to suppress the progression of nAR-negative BCa cells.

Materials and methods

Cell Culture and chemicals

BCa cell lines, J82, 5637, and UMUC3, were obtained from the American Type Culture Collection (Manassas, VA, USA). J82 and UMUC3 cells were maintained in DMEM and 5637 cells were maintained in RPMI-1640. The culture media were supplemented with 10% fetal bovine serum (FBS), antibiotics (100 units/ml penicillin, 100 mg/ml streptomycin), and 2 mM glutamine (Invitrogen, Grand Island, NY, USA), then cells grown in a humidified 5% CO₂ environment at 37 °C.

Lentivirus packaging

The standard calcium chloride transfection method was performed. The psAX2 packaging plasmid and pMD2G envelope plasmid, with the plasmid containing the knock-down/overexpression of the gene of interest (PLKO.1-vector, PLKO.1-shAR, PLKO.1-shSLC39A9, PLKO.1-shG_{αi}, PLKO.1-shMMP9, PWPI-vector, and PWPI-SLC39A9) were transfected into HEK293T cells for 48 h to generate the lentivirus supernatant, with oligo sequences listed in

Supplementary Table 2. The lentivirus supernatants were harvested through a 0.45 μm nitrocellulose filter and used immediately or frozen at -80 °C for later use.

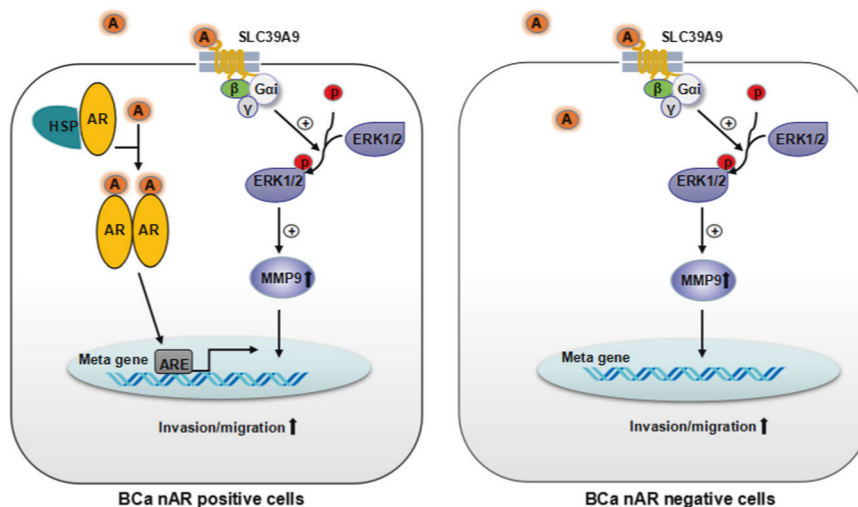
Wound-healing migration assay

The cells were seeded in 35-mm plates until confluent, then plates were scratched using a sterile pipette tip to generate a wound through the confluent monolayer. The cells were pretreated with/without T/DHT for 48 h after culturing for 2 days in charcoal-stripped FBS (10%) with phenol red-free media. Cells were analyzed and photographed with a microscope. Photographs of cell wounds were taken before and after 24 h treatment.

Transwell invasion assay

Cell invasion capacity was assessed by a matrigel invasion assay using matrigel (BD Corning, Corning, NY, USA) coated 8.0 μm filter membranes in transwell plates. The cells were pretreated with/without T/DHT for 48 h after culturing for 2 days in charcoal-stripped FBS (10%) with phenol red-free media. Cells (1×10^5) in 150 μL of serum-free media were plated onto each filter, with 750 μL of 10% charcoal-stripped serum-containing media placed in the lower chambers and then incubated for 24 h in a humidified environment at 5% CO₂ and 37 °C. After culture, filters were fixed with 4% paraformaldehyde on

Fig. 7 The cartoon model of DHT/SLC39A9/G α /MAPK/MMP9 axis signal pathways on nAR-positive and nAR-negative BCa cell migration and invasion



both sides, washed with PBS, and stained with crystal violet. Cells on the upper surface of the filters were removed with cotton swabs. Cells that had invaded to the lower surface of the filter were counted under the microscope. The relative invasion was determined by setting the number of invading cells in an ethanol control treated group as one.

RNA analysis by qRT-PCR

Total RNAs from transfected cells were isolated in two steps using Trizol reagent (Invitrogen). RNA (2 μ g) was reverse transcribed using Superscript III transcriptase (Invitrogen). The qRT-PCR was conducted using a Bio-Rad CFX96 system (primers were listed in Supplementary Table 3). SYBR green was applied to determine the mRNA expression level of a gene of interest. Expression levels were normalized to the mRNA expression of GAPDH.

Western blot analysis

Cells were lysed in RIPA buffer and total proteins (30 μ g) were separated on 10% SDS/PAGE gel and then transferred onto PVDF membranes (Millipore, Billerica, MA). After blocking membranes with 5% nonfat milk TBST solution, they were incubated with appropriate dilutions of specific primary antibodies (listed in Supplementary Table 4). The blots were incubated with HRP-conjugated secondary antibodies, and then visualized using the ECL system (Thermo Fisher Scientific, Waltham, MA).

Membrane-bound [35 S]-GTP γ S assay

Membrane [35 S]-GTP γ S binding assay was applied to evaluate the G protein activation. Cells were first incubated

with ETOH or 10 nM DHT for 45 min at 28 $^{\circ}$ C and harvest cell lysates on ice. The activated receptor exposed a binding site for G-protein complex binding. We added equal protein amounts of cell lysate and reacted with [35 S]-GTP γ S labeling mixture including a final concentration of 1 mM DTT, 0.1% (wt/vol) bovine serum albumin (BSA), 10 μ M GDP, and 0.1 nM [35 S]-GTP γ S. G α protein releases GDP and binds [35 S]-GTP γ S. G protein is then immunoprecipitated via stimulatory (Gas) and inhibitory (Gai) antibodies. The level of activated G α subunit was measured by 35 S isotope emission using the scintillation counter.

Co-immunoprecipitation

The lysates from J82 cells were incubated with the anti-SLC39A9 antibody for 16 h at 41 $^{\circ}$ C with agitation. Protein A/G-agarose beads were then added, and binding proteins were eluted. The eluted proteins were analyzed by western blotting with anti-SLC39A9 or anti-G α i antibodies.

Orthotopic mouse xenograft models

Male, athymic BALB/c, nude mice (4–6 weeks old, from NCI) were castrated before cell implantation. J82 cells transfected with luciferase reporter gene (pcDNA3.0-luciferase) were also transfected with PLKO-vector, PLKO-SCL39A9-shRNA, or PLKO-G α i-shRNA. The positive stable clones were selected and expanded in culture. Cells were harvested from 70 to 80% confluent cultures and washed once in serum-free DMEM medium and then resuspended in normal saline and mixed 1:1 with matrigel (BD Corning, Corning, NY, USA). Thirty-two mice were randomly divided into four groups (eight mice per group) for injection of cells and treatment as follows: PLKO-vector + EtOH (Mock), PLKO-vector + DHT, PLKO-SCL39A9-

shRNA+DHT, and PLKO-G_{ci}-shRNA+DHT. Mice were anesthetized by isoflurane. A small lower abdominal incision was made and the bladder was exposed. Cells were injected into the bladder wall using sterile syringes with a 30 gauge needle. The injection site was pressed with a cotton swab for 30 s and the incision was closed. DHT at 7 mg/kg (diluted in 20 μ l ethanol) or the same volume of ethanol was intraperitoneal injected (i.p. three times a week). The non-invasive In Vivo Imaging System (IVIS) (Caliper Life Sciences, Hopkinton, MA) was used to monitor tumor/metastases in live mice every week after tumor cell implantation following injection of 150 mg/kg Luciferin. Mice were killed after 6 weeks of implantation. The primary tumors and metastatic sites were further examined. Protocols for animal care and experimentation were approved by University of Rochester Medical Center's Animal Committee.

Tissue samples

A total of 63 BCa tissue samples were obtained from Xiangya Hospital, Central South University. These 63 patients, including 11 cases with <T2 tumors and 52 cases with T2–T4 tumors, were obtained by transurethral resection of bladder tumor or cystectomy. None of these patients received neoadjuvant chemotherapy before surgery. Details are shown in Supplementary Table 1. We compared mAR-SLC39A9 expression and clinicopathological features in these patients, including those with nAR-negative samples. These studies were approved by the Institutional Review Board of Xiangya Hospital.

IHC staining

IHC was performed on the samples from the human BCa tissues and mouse xenografted tumors. Briefly, the samples were fixed in 4% neutral buffered paraformaldehyde, embedded in paraffin, and cut into 5 μ m slices. After deparaffinization, hydration, and antigen retrieval, these sections were incubated with corresponding primary antibodies, incubated with biotinylated secondary antibodies (Vector Laboratories, Burlingame, CA, USA), and then visualized by VECTASTAIN ABC peroxidase system and 3, 3'-diaminobenzidine kit (Vector Laboratories, Burlingame, CA, USA). The slides were reviewed and scored by two experienced pathologists without any knowledge of the patient's outcome/history. The expression was assessed semi-quantitatively as follows: negative (–) < 5%, 5–25% (+, weak positive), 25–50% (++, moderate positive) and > 50% (+++, strong positive). Negative and weak positive expressions were defined as low expression, while moderate and strong positive expressions were defined as high expression.

Bioinformatic analysis of the TCGA database and Oncomine datasets

RNAseq Data from The Cancer Genome Atlas (TCGA) were retrieved from the TCGA database (<http://cancergenome.nih.gov>) using the UCSC Cancer Genome Brower (<https://genome-cancer.soe.ucsc.edu/>). Relative SLC39A9 mRNA expression in normal bladder tissues vs. BCa primary tumor tissues were compared. OS and DFS analysis for SLC39A9 mRNA expression in BCa patients were also analyzed. In addition, the expression level of SLC39A9 in BCa was analyzed using the Oncomine microarray datasets (www.oncomine.org). Search terms included “SLC39A9”, “BCa”, and “mRNA”. Finally, we compared the expression of SLC39A9 in bladder, bladder mucosa, and NMI BCa tissues of the Dyrskjot Bladder 3 dataset. And SLC39A9 expressions in NMI BCa and MI bladder urothelial carcinoma of the Sanchez-Carbayo Bladder 2 dataset were also acquired. All data are reported log₂ Median-Centered intensity in the ONCOMINE microarray datasets and converted to Median-Centered intensity.

Statistical analysis

Experiments were repeated independently at least three times with triplicate data points. Results are expressed as mean \pm SD. The Student's *t*-test, χ^2 -test, or Fisher's exact test and one-way analysis of variance were applied to determine statistical significance. A *P*-value of <0.05 was considered statistically significant.

Acknowledgements We thank Karen Wolf for help preparing the manuscript.

Funding This work was supported by NIH grant (CA155477), in part by Taiwan Ministry of Health and Welfare Clinical Trial and Research Center of Excellence (MOHW104-TDU-B-212-113002), the National Natural Science Foundation of China (81572523), and the Hunan Province Funds for Distinguished Young Scientists of China (2016JJ1026).

Author contributions J.B.C., F.J.C., S.Y.Y., X.B.Z., and C.S.C. designed the experimental protocols. J.B.C., F.J.C., Z.Y.O., C.R.S., C.P.H., Z.D.X., and Y.S. performed the studies. J.B.C., F.J.C., S.Y.Y., and Z.D.X. analyzed the data. J.B.C., F.J.C., C.R.S., C.P.H., Y.S., E.M., and C.S.C. wrote the manuscript with contributions from all of the other authors.

Compliance with ethical standards

Conflict of interest The authors declare that they have no conflict of interest.

Ethics approval and consent to participate This study was approved by the Xiangya Hospital, Central South University Ethics Committee. Signed informed consents were obtained from all the patients. And the

animal experiments were conducted strictly in accordance with the Animal Study Guidelines of University of Rochester Medical Center.

Publisher's note Springer Nature remains neutral with regard to jurisdictional claims in published maps and institutional affiliations.

References

- Antoni S, Ferlay J, Soerjomataram I, Znaor A, Jemal A, Bray F. Bladder cancer incidence and mortality: a global overview and recent trends. *Eur Urol*. 2017;71:96–108.
- Siegel RL, Miller KD, Jemal A. *Cancer Statistics, 2017*. *CA Cancer J Clin*. 2017;67:7–30.
- Kamat AM, Hahn NM, Efstathiou JA, Lerner SP, Malmstrom PU, Choi W, et al. Bladder cancer. *Lancet*. 2016;388:2796–810.
- Tan WS, Rodney S, Lamb B, Feneley M, Kelly J. Management of non-muscle invasive bladder cancer: a comprehensive analysis of guidelines from the United States, Europe and Asia. *Cancer Treat Rev*. 2016;47:22–31.
- Milowsky MI, Rumble RB, Booth CM, Gilligan T, Eapen LJ, Hauke RJ, et al. Guideline on muscle-invasive and metastatic bladder cancer (European Association of Urology Guideline): American Society of Clinical Oncology Clinical Practice Guideline Endorsement. *J Clin Oncol*. 2016;34:1945–52.
- Carneiro BA, Meeks JJ, Kuzel TM, Scaranti M, Abdulkadir SA, Giles FJ. Emerging therapeutic targets in bladder cancer. *Cancer Treat Rev*. 2015;41:170–8.
- Dobruch J, Daneshmand S, Fisch M, Lotan Y, Noon AP, Resnick MJ, et al. Gender and bladder cancer: a collaborative review of etiology, biology, and outcomes. *Eur Urol*. 2016;69:300–10.
- Siegel R, Ward E, Brawley O, Jemal A. Cancer statistics, 2011: the impact of eliminating socioeconomic and racial disparities on premature cancer deaths. *CA Cancer J Clin*. 2011;61:212–36.
- Chang C, Lee SO, Yeh S, Chang TM. Androgen receptor (AR) differential roles in hormone-related tumors including prostate, bladder, kidney, lung, breast and liver. *Oncogene*. 2014;33:3225–34.
- Chang CS, Kokontis J, Liao ST. Molecular cloning of human and rat complementary DNA encoding androgen receptors. *Science*. 1988;240:324–6.
- Li P, Chen J, Miyamoto H. Androgen receptor signaling in bladder cancer. *Cancers (Basel)*. 2017;9:E20.
- Miyamoto H, Zheng Y, Izumi K. Nuclear hormone receptor signals as new therapeutic targets for urothelial carcinoma. *Curr Cancer Drug Targets*. 2012;12:14–22.
- Ou Z, Wang Y, Liu L, Li L, Yeh S, Qi L, et al. Tumor micro-environment B cells increase bladder cancer metastasis via modulation of the IL-8/androgen receptor (AR)/MMPs signals. *Oncotarget*. 2015;6:26065–78.
- Tuygun C, Kankaya D, Imamoglu A, Sertcelik A, Zengin K, Oktay M, et al. Sex-specific hormone receptors in urothelial carcinomas of the human urinary bladder: a comparative analysis of clinicopathological features and survival outcomes according to receptor expression. *Urol Oncol*. 2011;29:43–51.
- Ide H, Inoue S, Miyamoto H. Histopathological and prognostic significance of the expression of sex hormone receptors in bladder cancer: a meta-analysis of immunohistochemical studies. *PLoS ONE*. 2017;12:e0174746.
- Sun YH, Gao X, Tang YJ, Xu CL, Wang LH. Androgens induce increases in intracellular calcium via a G protein-coupled receptor in LNCaP prostate cancer cells. *J Androl*. 2006;27:671–8.
- Sen A, Prizant H, Hammes SR. Understanding extranuclear (nongenomic) androgen signaling: what a frog oocyte can tell us about human biology. *Steroids*. 2011;76:822–8.
- Foradori CD, Weiser MJ, Handa RJ. Non-genomic actions of androgens. *Front Neuroendocr*. 2008;29:169–81.
- Miyamoto H, Yang Z, Chen YT, Ishiguro H, Uemura H, Kubota Y, et al. Promotion of bladder cancer development and progression by androgen receptor signals. *J Natl Cancer Inst*. 2007;99:558–68.
- De Toni L, Guidolin D, De Filippis V, Tesconi S, Strapazzon G, Santa Rocca M, et al. Osteocalcin and sex hormone binding globulin compete on a specific binding site of GPRC6A. *Endocrinology*. 2016;157:4473–86.
- Pi M, Parrill AL, Quarles LD. GPRC6A mediates the non-genomic effects of steroids. *J Biol Chem*. 2010;285:39953–64.
- Thomas P, Pang Y, Dong J, Berg AH. Identification and characterization of membrane androgen receptors in the ZIP9 zinc transporter subfamily: II. Role of human ZIP9 in testosterone-induced prostate and breast cancer cell apoptosis. *Endocrinology*. 2014;155:4250–65.
- Thomas P, Pang Y, Dong J. Membrane androgen receptor characteristics of human ZIP9 (SLC39A) zinc transporter in prostate cancer cells: androgen-specific activation and involvement of an inhibitory G protein in zinc and MAP kinase signaling. *Mol Cell Endocrinol*. 2017;447:23–34.
- Munnich N, Wernhart S, Hogstrand C, Schlomann U, Nimsky C, Bartsch JW. Expression of the zinc importer protein ZIP9/SLC39A9 in glioblastoma cells affects phosphorylation states of p53 and GSK-3beta and causes increased cell migration. *Biometals*. 2016;29:995–1004.
- Thal DM, Glukhova A, Sexton PM, Christopoulos A. Structural insights into G-protein-coupled receptor allostery. *Nature*. 2018;559:45–53.
- Tang X, Jin R, Qu G, Wang X, Li Z, Yuan Z, et al. GPR116, an adhesion G-protein-coupled receptor, promotes breast cancer metastasis via the Galphaq-p63RhoGEF-Rho GTPase pathway. *Cancer Res*. 2013;73:6206–18.
- Gao ZG, Jacobson KA. On the selectivity of the Galphaq inhibitor UBO-QIC: a comparison with the Galphai inhibitor pertussis toxin. *Biochem Pharm*. 2016;107:59–66.
- Berg AH, Rice CD, Rahman MS, Dong J, Thomas P. Identification and characterization of membrane androgen receptors in the ZIP9 zinc transporter subfamily: I. Discovery in female atlantic croaker and evidence ZIP9 mediates testosterone-induced apoptosis of ovarian follicle cells. *Endocrinology*. 2014;155:4237–49.
- Niu Y, Altuwaijri S, Lai KP, Wu CT, Ricke WA, Messing EM, et al. Androgen receptor is a tumor suppressor and proliferator in prostate cancer. *Proc Natl Acad Sci USA*. 2008;105:12182–7.
- Heinlein CA, Chang C. Androgen receptor in prostate cancer. *Endocr Rev*. 2004;25:276–308.
- Rosner W, Hryb DJ, Khan MS, Nakhla AM, Romas NA. Androgen and estrogen signaling at the cell membrane via G-proteins and cyclic adenosine monophosphate. *Steroids*. 1999;64:100–6.
- Lieberherr M, Grosse B. Androgens increase intracellular calcium concentration and inositol 1,4,5-trisphosphate and diacylglycerol formation via a pertussis toxin-sensitive G-protein. *J Biol Chem*. 1994;269:7217–23.
- Pi M, Quarles LD. GPRC6A regulates prostate cancer progression. *Prostate*. 2012;72:399–409.
- Thomas P, Converse A, Berg HA. ZIP9, a novel membrane androgen receptor and zinc transporter protein. *Gen Comp Endocrinol*. 2018;257:130–6.
- Izumi K, Taguri M, Miyamoto H, Hara Y, Kishida T, Chiba K, et al. Androgen deprivation therapy prevents bladder cancer recurrence. *Oncotarget*. 2014;5:12665–74.
- Shiota M, Yokomizo A, Takeuchi A, Imada K, Kiyoshima K, Inokuchi J, et al. Secondary bladder cancer after anticancer therapy for prostate cancer: reduced comorbidity after androgen-deprivation therapy. *Oncotarget*. 2015;6:14710–9.

37. Goldsmith ZG, Dhanasekaran DN. G protein regulation of MAPK networks. *Oncogene*. 2007;26:3122–42.
38. Wang JL, Yang MY, Xiao S, Sun B, Li YM, Yang LY. Downregulation of castor zinc finger 1 predicts poor prognosis and facilitates hepatocellular carcinoma progression via MAPK/ERK signaling. *J Exp Clin Cancer Res*. 2018;37:45.
39. Huang B, Xiao E, Huang M. MEK/ERK pathway is positively involved in hypoxia-induced vasculogenic mimicry formation in hepatocellular carcinoma which is regulated negatively by protein kinase A. *Med Oncol*. 2015;32:408.
40. Liu Q, Zou R, Zhou R, Gong C, Wang Z, Cai T, et al. miR-155 regulates glioma cells invasion and chemosensitivity by p38 isforms in vitro. *J Cell Biochem*. 2015;116:1213–21.